Chapter 9

Use of Polyurethane Foam in Orthopaedic Biomechanical Experimentation and Simulation

V. Shim, J. Boheme, C. Josten and I. Anderson

Additional information is available at the end of the chapter

http://dx.doi.org/10.5772/47953

1. Introduction

Biomechanical experimentation and computer simulation have been the major tool for orthopaedic biomechanics research community for the past few decades. In validation experimentations of computer models as well as *in vitro* experimentations for joint biomechanics and implant testing, human cadaver bones have been the material of choice due to their close resemblance to the *in vivo* characteristics of bones. However, the challenges in using cadaveric bones such as availability, storage requirements, high cost and possibility of infection have made synthetic bone analogs an attractive alternative.

There are a variety of synthetic bone materials available but polyurethane foam has been used more extensively in orthopaedic experiments, especially in fracture fixation testing. The foams are produced by a polymerization reaction with a simultaneous generation of carbon dioxide by the reaction of water and isocyanate. The resultant product is a closed cell structure, which is different from the open porosity of cancellous bone. However the uniformity and consistency in their material properties make rigid polyurethane ideal for comparative testing of various medical devices and implants.

Therefore we have extensively used synthetic bones made of polyurethane foam in various orthopaedic biomechanical researches from optimization of bone graft harvester design to acetabular fractures and the stability of osteosynthesis. We identified important design parameters in developing bone graft harvester by performing orthogonal cutting experiment with polyurethane foam materials. We also validated the fracture prediction capability of our finite element (FE) model of the pelvis with a validation experiment with polyurethane foam pelvis. We also performed in vitro experimentation to compare the stability of different types of osteosynthesis in acetabular fractures and used this result again to validate our fracture fixed pelvis model. These results as well as reports from others that

highlight the use of polyurethane in orthopaedic biomechanical experiment will be included in this chapter.

Specifically, there will be three sections in this chapter. The first section will describe the basic material properties of rigid polyurethane foam. We will especially highlight the similarities and differences between the foam and human bone. The second section will then present the review of the literature focusing on the use of polyurethane foam in biomechanical experimentations. We will conclude the chapter with our use of polyurethane foam in bone grafting harvester design, fracture predictions and stability testing of osteosynthesis.

2. Basic material properties of rigid polyurethane foam

Polyurethanes are characterized the urethane linkage (-NH-C(=O)-O-) which is formed by the reaction of organic isocyanate groups with hydroxyl groups as shown below

$$R\text{-}NCO + R'\text{-}OH = R\text{-}NH\text{-}C(=O)\text{-}O\text{-}R'$$

Polyurethanes can be turned into foam by means of blowing agents such as water. The cells created during the mixing process are filled and expanded with carbon dioxide gas, which is generated when water reacts with isocyanate group. The result is a closed foam structure, which is a cellular solid structure made up of interconnected network of solid struts or plates which form the edges and faces of cells. Thanks to its desirable material properties that give versatility and durability to the material, polyurethane has become one of the most adaptable materials that it is found everywhere such as carpet, sofa, beds, cars to name a few.

One unlikely place, however, is inside human body, that is human cancellous or spongy bone. The macroscopic structure of cancellous bone consists of a network of interconnecting rods and plates that forms complex struts and columns. Although this structure has strictly speaking open porosity structure, the overall macroscopic structure shows close resemblance to the closed foam structure of polyurethane foam (Figure 1)

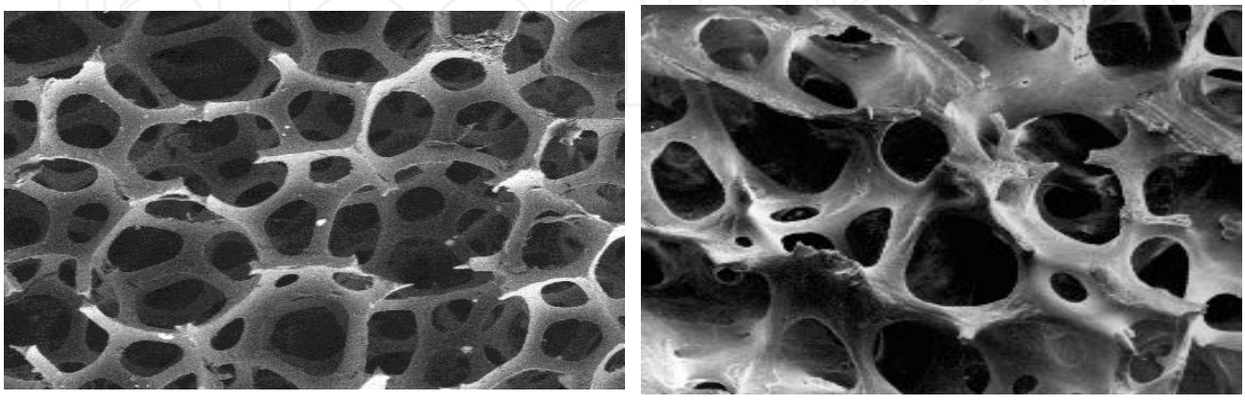

Polyurethane foam microscopic structure

Cancellous bone microscopic structure

Figure 1. Microstructures of cancellous bone and polyurethane foam.

The stress-strain curve of polyurethane foam exhibits similar pattern as cancellous bone. Figure 2 shows a schematic compressive stress-strain curve for polyurethane foams which shows three regions; firstly they show linear elasticity at low stresses followed by a long plateau, truncated by a regime of densification at which the stress rises steeply (Gibson and Ashby, 1988). Linear elasticity is controlled by cell wall bending while the plateau is associated with collapse of the cells by either elastic buckling or brittle crushing. When the cells have almost completely collapsed opposing cell walls touch and further strain compresses the solid itself, giving the final region of rapidly increasing stress.

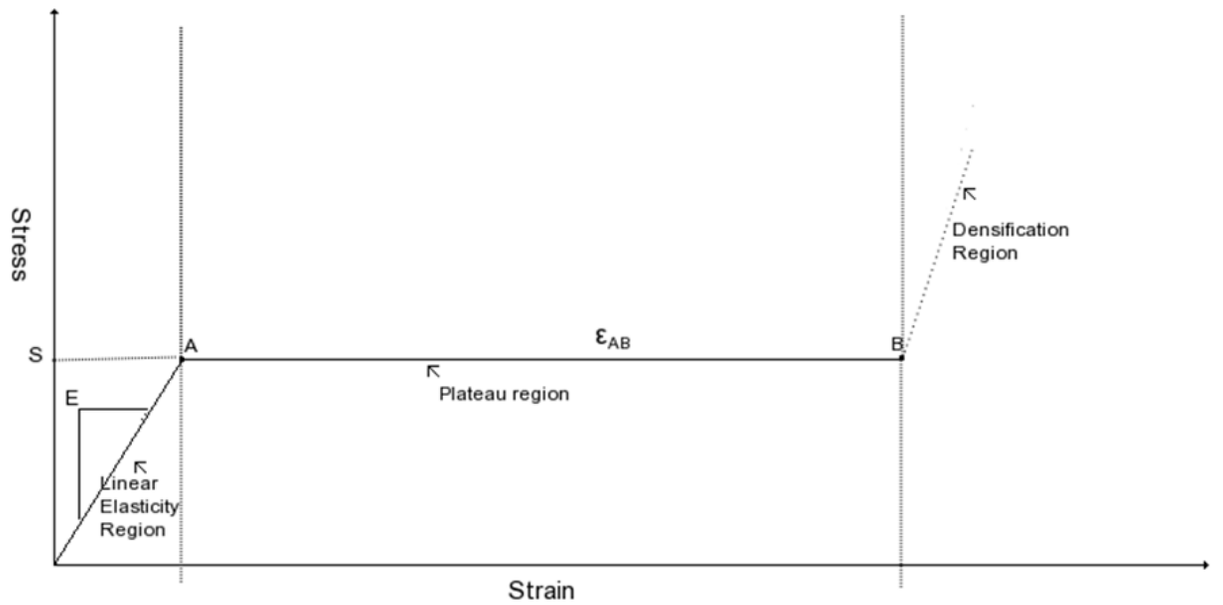

Figure 2. Typical compressive stress-strain curve of polyurethane foam

The compressive stress-strain curve of cancellous bone has the similar three regimes of behaviour (Figure 3). Firstly the small strain, linear elastic region appears which is mainly from the elastic bending of the cell walls. Then the linear-elastic region ends when the cells begin to collapse and progressive compressive collapse gives the long horizontal plateau of the stress-strain curve which continues until opposing cell walls meat and touch, causing the stress rise steeply.

Such similarities have made polyurethane (PU) foams as popular testing substitutes for human cancellous bones and many researchers have quantitatively characterized material properties of polyurethane foam to investigate the suitability and usefulness of PU foams as bone analog. Szivek, Thomas and Benjamin (Szivek et al., 1993)conducted the first study on mechanical properties of PU foams with different microstructures. Compression testing was done to identify elastic modulus and compressive strength. The same group conducted further studies with three compositions of PU foams and evaluated their properties as well(Szivek et al., 1995). Thompson and co-workers(Thompson et al., 2003) analyzed compressive and shear properties of commercially available PU foams. They tested samples of four grades of rigid cellular foam materials and found out that elastic

behaviour was similar to cancellous bones and an appropriate density of PU foams can be determined for a particular modulus value. However the shear response showed some discrepancy and concluded that caution is required when simulating other behaviours than elastic behaviour with these foams. Calvert and coworkers (Calvert et al.) evaluated cyclic compressive properties of PU foams and examined the mechanical properties in terms of microstructural features. They found that microstructural properties such as cell size and volume were uniform and increased with decreasing density. And their cyclic testing revealed hysteresis in the low density foams but consistent modulus up to 10 cycles.

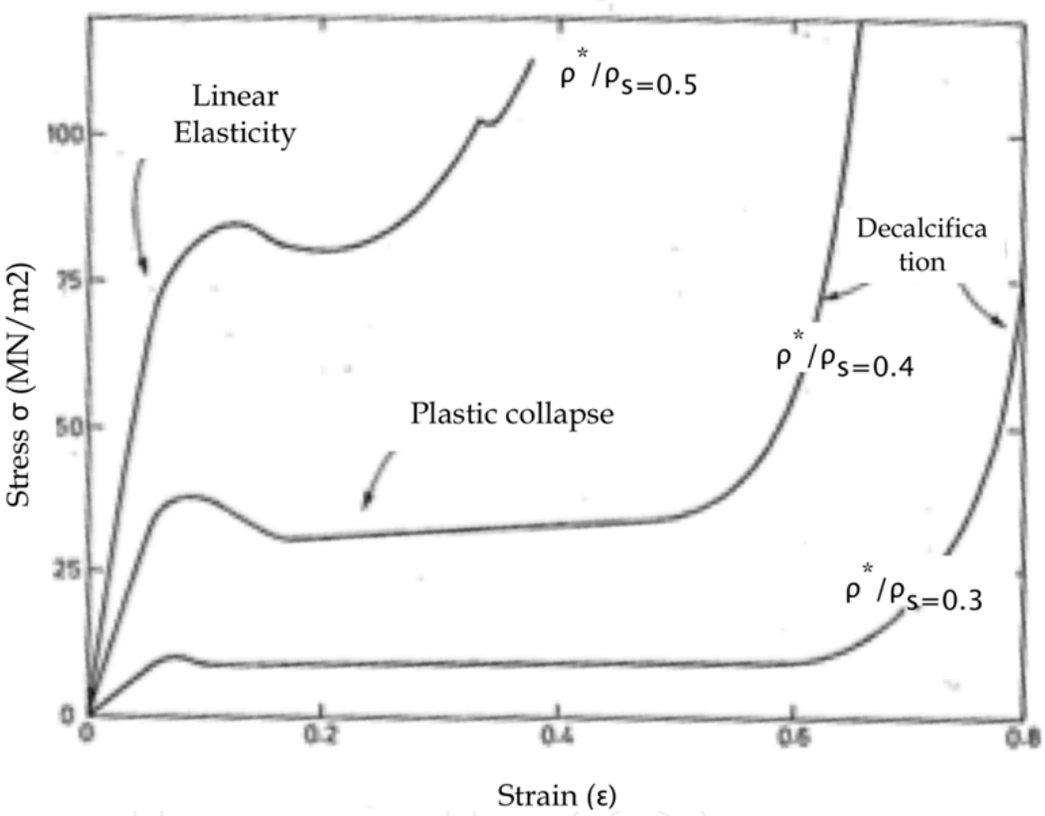

Figure 3. Compressive stress-strain curves for several relative densities (ϱ^*/ϱ_s)of wet cancellous bone (modified from Figure 11-5 in Gibson and Ashyby, 1997)

As the use of PU foams in orthopaedic implant testing and their use as bone analogs increased, the American Society for Testing and Materials (ASTM) developed ASTM F1839-97, "Rigid polyurethane foam for use as a standard material for testing orthopaedic devices and instruments." The aim of this standard is to provide a method for classifying foams as graded or ungraded based on the physical and mechanical behaviour with a given density. This standard has been revised twice since 1997 when it was originally introduced in order to include a wide range of properties and nominal densities(American Society for Testing and Materials, 2008a). As such the number of studies that used PU-foam in testing implant materials and function has increased dramatically after the introduction of the standard. The next section will give review of those studies.

3. The use of PU foams in orthopaedic implant testing

The number and variety of implants for osteosynthesis and joint replacement has increased dramatically over the past few decades along with the use of biomechanical testing of these implants to evaluate their performance. The most obvious material of choice will be fresh or embalmed cadaveric human or animal bones as they have the unique viscoelastic properties and internal structures of real bone. However such studies are often beset with a number of other problems such as issues in handling biological samples and huge variety in size, shape and material properties even in matched pairs to name a few. If reproducibility of experiments is important and comparable not absolute results are required, synthetic bones made from PU-foam can provide a great alternative to the real bones (Figure 4).

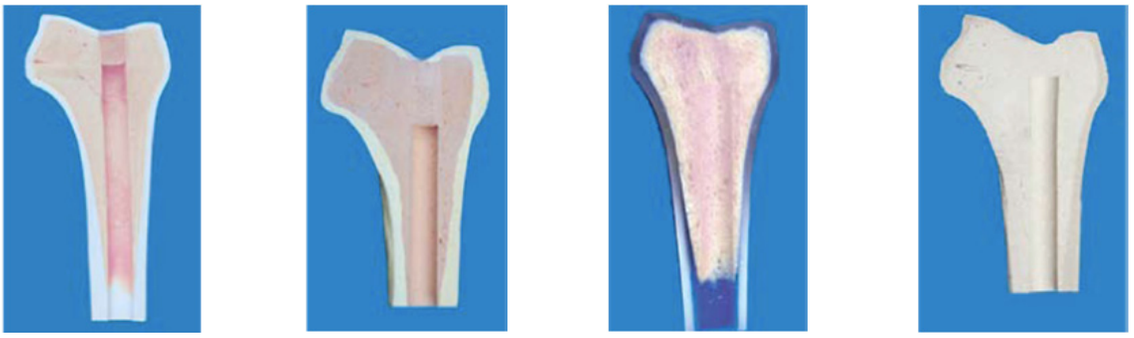

(a) plastic cortical shell with cellular PU-foam inside

(b) rigid PU-foam cortical shell with cellular PU-foam inside

(c) transparaent plastic cortical shell with cellular PU-foam inside

(d) Solid PU-foam throughout

Figure 4. Various synthetic bone material combinations with different types of PU foams and plastics (from www.sawbones.com)

The major use of PU foam blocks is comparatives studies for quantitatively measuring some important functional parameters of orthopaedic implants such as pull out strength, stability and stiffness. Bredbenner et al. (Bredbenner and Haug, 2000) investigate the suitableness of synthetic bone made of PU-foam in testing rigidity of fracture fixations by comparing pull out strength from cadaveric bones, epoxy red oak and PU foams. They found out that PU-foam bone substitutes generated comparable results to cadaveric bones, concluding that PU-foams can be used in mechanical investigation of human bones.

Indeed many researchers have used PU-foam in comparative studies measuring pullout strength of fixation screws. Calgar et al.(Caglar et al., 2005) performed biomechanical comparative studies of different types of screws and cables using Sawbone models and found out that the load to failure of screws was significantly greater than that of the cables. Farshad et al. (Farshad et al., 2011)used PU foam blocks to test bone tunnels drilled during anterior cruciate ligament reconstruction. They found that screw embossed grafts achieved higher pull out strengths. Krenn et al. (Krenn et al., 2008)investigated the influence of thread design on screw fixation using PU-foam blocks with different densities.

PU-foams are also extensively used in biomechanical studies for finding optimal surgical parameters in orthopaedic surgeries. For example, osteotomy is a surgical procedure where a bone is cut to shorten or lengthen to rectify abnormal alignment. One variation of that technique is Weil osteotomy where the knuckle bone in the foot is cut to realign the bones and relieve pain. There are two separate independent studies on Weil osteotomy involving PU-foams and cadaver bones. Melamed et al. (Melamed et al., 2002) used 40 PU-foams to find the optimal angle for the osteotomy and found that an angle of 25° to the metatarsal shaft give the best result. This result was confirmed a year later by Trnka et al. (Trnka et al., 2001)who performed the similar study on fresh frozen cadaver feet. They also found that the range between 25°-35° give the optimal results, confirming that the use of PU-foams in such studies. Nyska et al. (Nyska et al., 2002) analyzed osteotomy for Bunion deformity using 30 PU-foams and found that displacement osteotomies provided good correction for middle and intermediate deformity. Acevedo et al. (Acevedo et al., 2002) compared five different first metatarsal shaft osteotomies by analyzing the relative fatigue endurance. They used 74 polyurethane foam synthetic bones to determine the two strongest of the five osteotomy techniques and they found that Chevron and Ludloff osteotomies showed superior endurance than the other techniques.

Nasson and coworkers (Nasson et al., 2001)used eight foam specimens for tibia and talus to evaluate the stiffness and rigidity of two different arthrodesis techniques where artificial joint ossification is induced between two bones either with bone graft or synthetic bone substitutes. They performed arthrodesis on these artificial bones made up of PU-foams and tested rotation and bending strength and recommended that the use of crossed screws for the strength, simplicity , speed and minimal tissue dissection.

Another interesting development in the use of PU foam in orthopaedic biomechanics is the development of so called composite bones. Since PU foam closely resembles cancellous bone structure and properties, a composite material made up of epoxy resin with fibre glass along with PU foam was used to create a synthetic bone where cortical and cancellous bone materials are simulated with epoxy resin and PU foam respectively (Figure 5). Zdero et al (Zdero et al., 2007, Zdero et al., 2008) tested the performance of these composite bones by measuring bone screw pullout forces in such composite bones and comparing them with cadaver data from previous literature. They found out that composite bones provide a satisfactory biomechanical analog to human bone at the screw-bone interface.

When such composite bone material is shaped according to the actual bony shapes of human bones such as femur and tibia, they can be a great alternative for cadaver bones in research and experiment. Since they closely mimic both geometry and material properties of actual bones and yet have consistency that is lacking in cadaver bones, they can lower variability significantly, offering a more reliable testing bed. Composite replicates of femur and tibia were first introduced in 1987 and then have undergone a number of design changes over the years. The currently available composite bones are fourth-generation composite bones where a solid rigid PU-foam is used as cancellous core material while a

mixture of glass fibres and epoxy resin was pressure injected around the foam to mimic cortical bone. Chong et al. (Chong et al., 2007a, Chong et al., 2007b) performed extensive mechanical testing with these synthetic bones and found out that the fourth-generation material has better fatigue behavior and modulus, strength and toughness behaviours a lot closer to literature values for fresh-frozen human bones than previous composite bones. Heiner (Heiner, 2008) tested stiffness of the composite femurs and tibias under bending, axial and torsional loading as well as measuring longitudinal strain distribution along the proximal-medial diaphysis of the femur. She found out that the fourth-generation composite bones average stiffness and strains that were close to values for natural bones (Table 1). Papini et al.(Papini et al., 2007) performed an interesting study where they compared the biomechanics of human cadaveric femurs, synthetic composite femurs and FE femur models by measuring axial and torsional stiffness. They found that composite femurs represents mechanical behaviours of healthy rather than diseased femur (e.g. osteoporosis), hence caution is required in interpreting the data from experiment with composite bones.

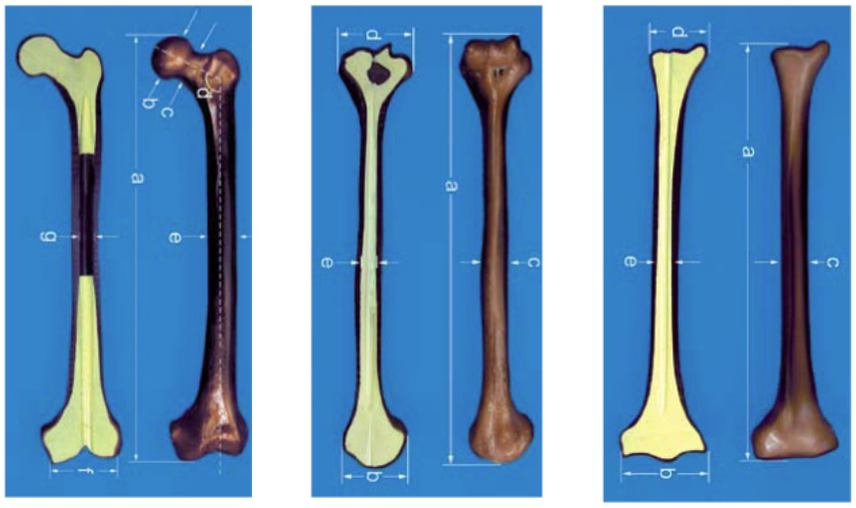

(a) Femur (b) Humerus (c) Tibia

Figure 5. Various composite bones made up of PU-foam core covered with a cortical shell of short fiber filled epoxy (from www.sawbones.com)

Property	Bone Type	Value
Anterior flexural rigidity (N m^2)	Natural	317
	Composite	241
Lateral flexural rigidity (N m^2)	Natural	290
	Composite	273
Axial stiffness (N/μm)	Natural	2.48
	Composite	1.86
Torsional rigidity (N m^2/deg)	Natural	4.41
	Composite	3.21

Table 1. Structural properties of natural human and 4th generation femurs (modified from Table 2 of (Heiner, 2008))

The advert of such biomechanically compatible bone analog greatly widened the use of PU-foam in orthopaedic biomechanics experiments as more mechanically meaningful parameters such as strength and surface strains were possible to be introduced in the design of the experiment.

Agneskirchner et al. (Agneskirchner et al., 2006) investigated primary stability of four different implants for high tibial osteotomy with composite bones and found that the length and thickness as well as the rigidity of the material strongly influence the load to failure of tibial osteotomy. Gulsen et al. (Gulsen et al.) used composite bone in testing biomechanical function of different fixation methods for periprosthetic femur fractures and compared the yield points of these techniques. Cristofolini et al. (Cristofolini et al., 2003) performed in vitro mechanical testing with composite femurs to investigate difference between good design and bad design in total hip replacement femoral stems. They placed two different implants (one good design and the other bad design) to synthetic femurs and applied one million stair climbing loading cycles and measured interface shear between the stem and cement mantle to see the result of long term performances. Their set-up involving composite bones was sensitive enough to detect the result of design difference and was able to predict long term effects of different implant designs. Simoes et al. (Simoes et al., 2000) investigated the influence of muscle action on the strain distribution on the femur. They measured strain distributions for three loading conditions that involve no muscle force, abductor muscle force only and then 3 major muscle forces in the hip. They placed 20 strain gauges on the composite femur and applied muscle and joint forces accordingly. They found out that strain levels were lower when muscle forces were applied than when only joint reaction force was used, indicating that the need to constrain the femoral head to reproduce physiological loading conditions with joint reaction force only.

As discussed up till now, the use of PU-foam based material is almost limitless and the list discussed here is by no means an exhaustive survey of the use of PU-foam based materials in orthopaedic experiment. However, our group has also been working with the PU-foam materials in our orthopaedic biomechanics extensively. The following chapters give summary of these works.

4. Use of PU-foams in device and implant testing for bone grafting and acetabular fractures

4.1. Identification of optimal design parameters in bone grafting tools with PU-foams

Bone grafting is a reconstructive orthopaedic procedure in which a bone substitute is used to fuse broken bones and to repair skeletal defects (Arrington et al., 1996, Lewandrowski et al., 2000). Bone grafting is performed worldwide around 2.2 million times per year, with approximately 450 000 procedures in the United States alone (Russell and Block, 2000). Most popular method is autograft where the graft material is extracted from the patient itself. The graft can be harvested from the patient's femur, tibia, ribs and the iliac crest of the

pelvis(Betz, 2002). Autograft has the advantages of being histocompatible and non-immunogenic, it eliminates the risk of transferring infectious diseases and has osteoinductive and osteoconductive properties (Arrington et al., 1996). However, the harvesting procedure often requires a second incision to extract the graft from the donor site, which can extend operation time by up to 20 min (Russell and Block, 2000). The ensuing donor site morbidity is regarded as "a serious postoperative concern for both patient and surgeon" (Silber et al., 2003). Ross et al. (Ross et al., 2000) reported an overall complication rate of 3.4–49%, of which 28% suffered persistent pain, which can last as long as 2 years and often exceeds the pain from the primary operation.

The reason for donor site pain remains unclear, however, it might be proportional to the amount of dissection needed to obtain the graft (Kurz et al., 1989). Conventional bone grafting tools usually require great exposure of the donor site with accompanied trauma to nerves and muscles. Damage to nerves and muscles may be reduced by using minimally invasive bone grafting techniques (Russell and Block, 2000), which shorten the incision length by approximately 60%, reduce the amount of dissection and are roughly two times faster than conventional methods (Burstein et al., 2000). Minimally invasive tools are usually rotational cutting tools, which include trephines, bone grinders (Burstein et al., 2000) and bone graft harvesters as depicted in Figure 6 A.

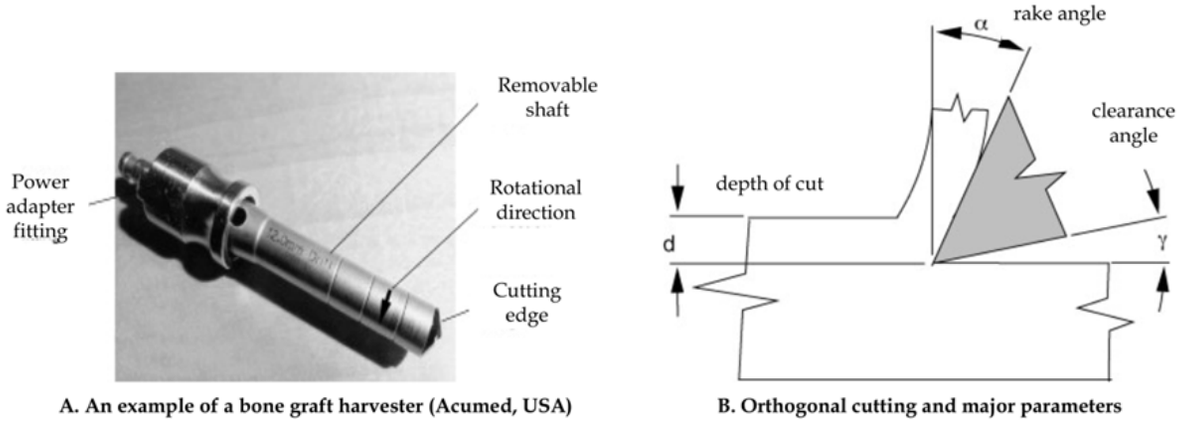

Figure 6. Bone graft harvester and its major parameters

The harvester collects the graft, i.e. bone chips consisting of cancellous bone fragments and bone marrow, in its barrel as it turns and penetrates deeper into the bone. Despite the advantages of using minimally invasive tools such as the bone graft harvester, cell morbidity is yet unavoidable, because both fracturing of the bone architecture and heat generation accompany every bone cutting process. However, mechanical and thermal damage could be reduced by improving tool geometry and by applying appropriate cutting parameters.

Many researchers have studied various cutting operations, such as orthogonal cutting (Jacobs et al., 1974), drilling (Saha et al., 1982, Natali et al., 1996) milling (Shin and Yoon, 2006) and sawing (Krause et al., 1982), in order to identify some of the critical parameters that influence heat generation and to gain an overall understanding of bone cutting

mechanisms. For a bone graft harvester, these parameters are the rake and point angles of tool, the rotational speed and the feed rate (Figure 6 B).

The influence of such parameters can be measured by characterizing chip types formed when cutting the bone. Smaller chips imply more fracturing per volume of bone material collected and due to the linkage between fracturing of the bone architecture and cell morbidity, and larger chips are believed to act as "life rafts" for the bone cells and will increase the rate of survival for embedded living cells. We have conducted two-part study where we identified various chip types during orthogonal cutting process(Malak and Anderson, 2008, Malak and Anderson, 2005).

In Part I (Malak and Anderson, 2005), we used polyurethane foams of various densities and cell sizes to investigate chip formation and surface finish. An optical arrangement made up of dynamometer, microscope and camera system (Figure 7) was used to visually record the cutting process, while horizontal and vertical cutting forces were measured. A total of 239 measurement were performed using rake angles of 23°, 45° and 60° with depths of cut from 0.1 to 3 mm (increments of 0.1 and 0.2 mm). Cutting events were observed on the video and then linked to simultaneous force events by merging both sets of data into a combined video stream, generating force plot images.

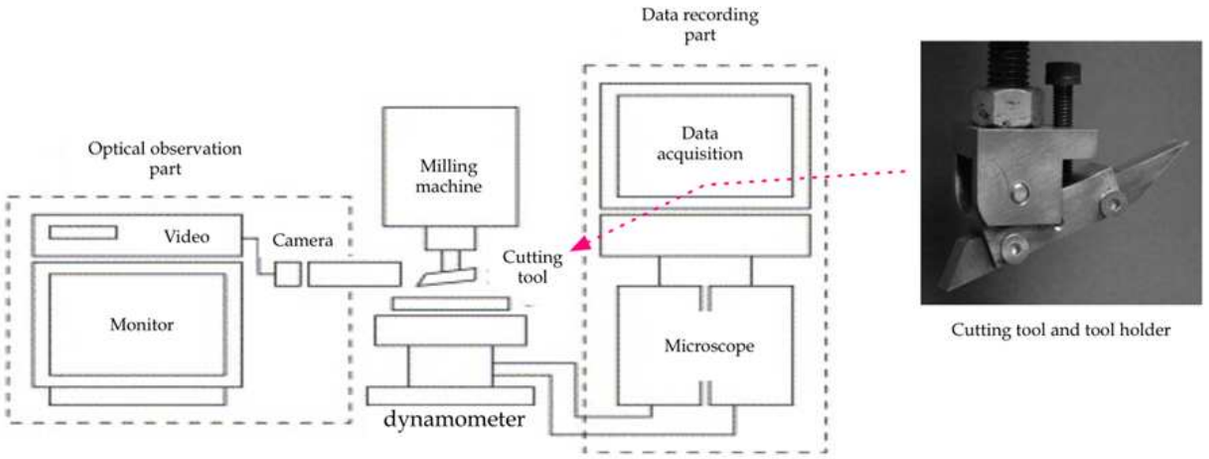

Figure 7. Experimental set-up for measuring chip formation during orthogonal cutting procedure

Three types of cutting response were identified and categorized as 1) surface fragmentation; 2) continuous chip formation; 3) discontinuous chip formation depending on tool rake angle, depth of cut, foam density and cell size (Figure 8). Surface fragmentation was associated with cutting depth less than the PU-foam cell size. By cutting an order of magnitude of the cell size deeper, continuous chips were produced, which is a desirable feature whenever good surface finish after cutting is desired as in the case of bone harvester. A large rake angle (60°) was also inductive of continuous chip formation. Discontinuous chip formation was associated with 1) foam compaction followed by chevron shaped chip; 2) crack propagation in front of the tool. Compaction of the foam could be minimized by using a tool with a large rake angle and normal cut depth.

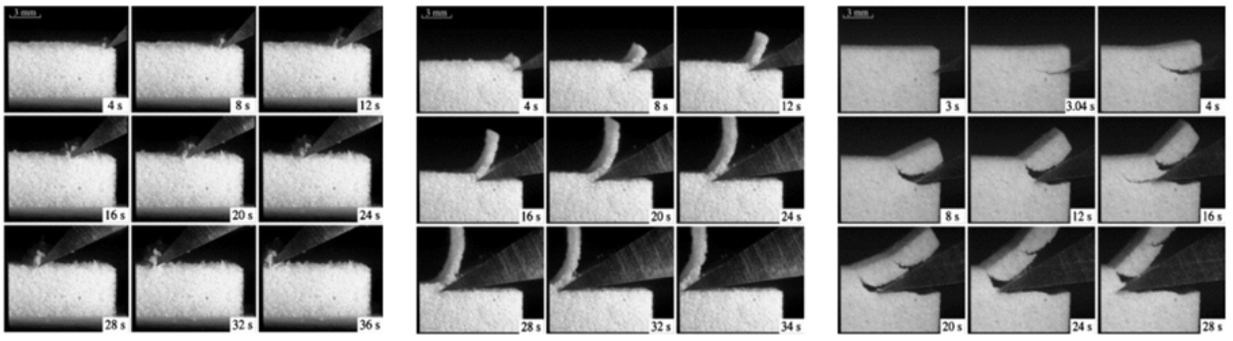

Figure 8. Various chip types formed during orthogonal cutting of polyurethane foams of various densities

The same experiment was repeated with bovine fresh cancellous bone(Malak and Anderson, 2008) from the patella, the femur and the iliac crest. Similar orthogonal cutting experiments were conducted using the same device used in Part I to identify major parameters that influence the formation of chips after cutting. Three groups of experiments were done where the effect of the depth of the cut, rake angle and cutting speed. Similar chip types as the experiment with PU-foams in Part I were observed which were found to be dependent on rake angle and depth of cut (Figure 9).

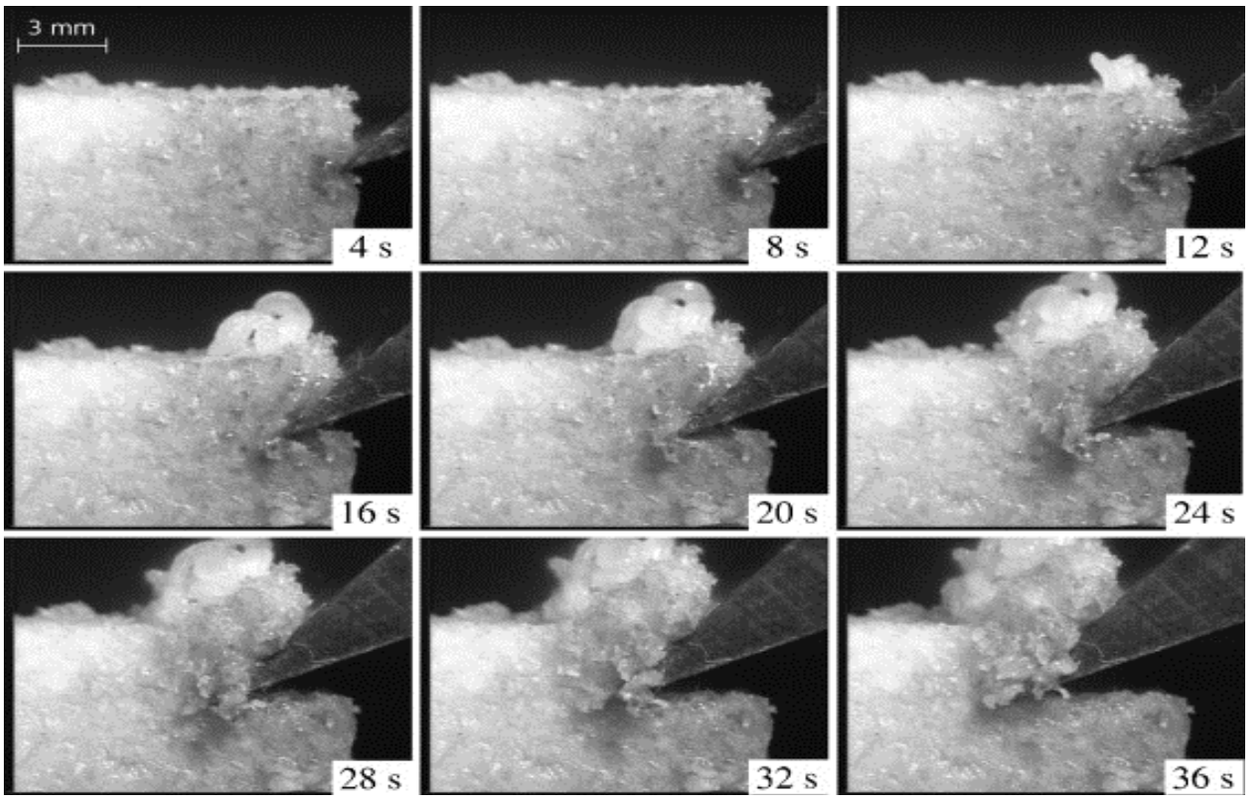

Figure 9. Chip foramtion during orthogonal cut of cancellous bone.

When the results from cancellous bone were compared with those from PU-foams, both showed surface fragmentation, continuous and discontinuous chip formations. During polyurethane foam cutting, chip types were influenced by rake angle and depth of cut. Bone cutting showed similar trend, however, resulting chip type were mainly influenced by the tool rake angle. We also identified the depth of cut that marked the transition from surface fragmentation to continuous or discontinuous chip types. In PU-foams, such a transition is indicated by a change in cutting forces. A similar trend was observed in bone; a depth of cut of 0.5 mm ~ 0.8 mm led to continuous or discontinuous chips. These values approximately correspond to the trabecular separation values. This is in accordance with our findings during the cutting of polyurethane foam, where depths of cut had to reach values of the foam cell size diameter in order to be either continuous or discontinuous.

Therefore polyurethane foam was successfully used in identifying optimal parameters for designing minimally invasive bone graft harvester. The next section will describe how PU-foam based synthetic bone was used in FE modeling of hip fracture.

4.2. Development and validation of finite element fracture predictions with PU-foam based synthetic bones

Acetabular fractures are one of the big challenges that trauma surgeons face today. Despite the great stride made in treating this fracture in the past few decades, one medical text book states that "fractures of the acetabulum remains an enigma to the orthopaedic surgeon(Tile et al., 2003)." The main reason for this difficulty lies on the complexity of acetabular fractures. Acetabular fractures are usually a result of indirect trauma where the major impact is transmitted via the femur after a blow to the greater trochanter, to the flexed knee or to the foot with the knee extended (Ruedi et al., 2007). Moreover acetabular fractures are dependent on a number of variables such as the type of force that caused the fracture, the direction of displacement, the damage to the articular surface as well as the anatomical types of the fracture (i.e. the shapes of the fragments). The relative rareness of acetabular fractures makes matters worse since general orthopaedic surgeons may not gain wide experience with them.

The past researches on acetabular fracture can be broadly divided into two categories. The first is experimental studies where the stability of different acetabular fracture fixation techniques was investigated with in-vitro mechanical experiments (Goulet et al., 1994, Konrath et al., 1998a, Konrath et al., 1998b, Olson et al., 2007). There are also clinical studies that examined the effectiveness and longer-term results of different fracture fixation techniques (Borrelli et al., 2005, Cole and Bolhofner, 1994, Giannoudis et al., 2005). Finite element (FE) models can enhance greatly the body of knowledge obtained from such experimental and clinical studies. FE models can overcome the limitations of in-vitro experimental studies because they can be used to simulate the behaviour of the fractured acetabulum under physiological loading conditions that include muscle forces. FE models can also elevate the results from clinical studies into a new dimension as they can be used to predict the outcome of particular fixation techniques after the surgery. If the model performance in fracture prediction is validated, it can be used to evaluate various fixation

techniques depending on their fracture types. The problem is how to validate the model. If cadaver bone is to be used, the issue of sample variability and the requirement of ethics approval, special storage and high cost need to be resolved first. Therefore the aim of this study is to develop a finite element model of the pelvis that can accurately predict the fracture load and locations of acetabular fractures and validate its performance with synthetic PU-foam based bones(Shim et al., 2010).

4.2.1. Fracture experiment with PU-foam synthetic pelvic bones

Ten synthetic male pelves made with polyurethane foam cortical shell and cellular rigid cancellous bone (Full Male Pelvis 1301-1, Sawbones, Pacific Research Laboratories, INC, Washington, WA, USA) were used for fracture experiment. A similar set-up as (Shim et al., 2008) was used where the pelvis was placed upside down in a mounting pane filled with acrylic cement. Two different loading conditions – seating (or dashboard) fracture and fall from standing fracture – were tested. When the angle (α) between the vertical line and the line formed by joining the pubic tubercle and the anterior superior point of the sacrum (Figure 10) was 30 °, the whole set-up mimicked the standing position, hence simulating standing fracture. When the angle α was raised to 45°, the set-up mimicked the position of the pelvis when seated, hence simulating seating fracture. Force was exerted from the femoral head attached to the crosshead of the Instron machine (Instron 5800 series, Norwood, MA, USA). The femoral head was also from a matching Sawbone femur (Large Left femur 1130, Sawbones, Pacific Research Laboratories, INC, Washington, WA, USA) to the pelvis used. The femur was first chopped at the neck region and then attached to a custom made holding device connected to the crosshead of the Instron machine (Figure 10). The femoral head was dipped into liquid latex to ensure a complete and stable seating of the femoral head to the acetabulum. The force was applied from the femoral head to the acetabulum at a constant speed of 40N/s until failure. Total ten pelves were used for testing. Five were tested for standing fracture and the rest was tested for seating fracture. The fracture loads and patterns were recorded for comparison with finite element simulations

Figure 10. Photos of the experiment: The photo on the left shows the angle alpha that determined seating or standing positions; the center photo shows the close-up of the chopped femoral head attached to the holding device that goes into the crosshead of the Instron machine; the photo on the right shows the overall set-up.

4.2.2. Finite element analysis of PU-foam based synthetic pelvis

The Sawbone pelvis used in the experiment was CT scanned (Philips Brilliance 64, Philips). Each CT image was manually segmented and a finite element model of the hemi pelvis was generated using the previously validated procedure (Shim et al., 2007, Shim et al., 2008)(Figure 11). Our model is both geometrically and materially non-linear. Geometric non-linearity was achieved by using finite elasticity governing equations rather than linear elasticity approximations (Shim et al., 2008). Material non-linearity was incorporated in a similar manner as in (Keyak, 2001). In our model, the material behaviour of the synthetic PU-foam based pelvis was divided into two regions – 1) an elastic region with a modulus E; 2) perfectly plastic regions with a plastic strain εAB (Figure 11) according to the material behaviour of polyurethane materials(Thompson et al., 2003). The value for εAB was obtained from the specifications provided by the manufacturer (Pacific Research Laboratories, INC, Washington, WA, USA).

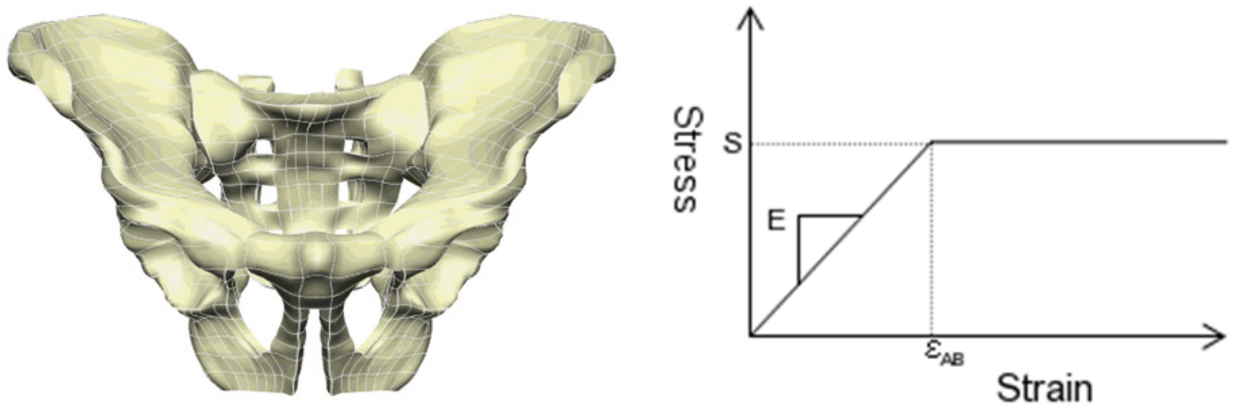

Figure 11. FE model and it nonlinear material behaviour. The polyurethane foam material behavior was represented by an elastic region with modulus E until stress S, followed by a perfectly plastic region with plastic strain εAB.

Two materials were incorporated in our model – 1) solid polyurethane foam that mimicked the cortical bone property; 2) cellular rigid polyurethane foam for cancellous bone. The material properties for the two polyurethane foams are given in Table 2.

	Density (g/cc)	Strength (MPa)	Modulus (MPa)
Solid polyurethane foam	0.32	8.8	260
Cellular polyurethane foam	0.16	2.3	23

Table 2. Material properties of solid and cellular polyurethane foam

The previously developed algorithm that determines cortical thickness was used to distinguish between solid polyurethane and cellular polyurethane foam regions from CT scans. We used Gauss points inside the mesh to assign material properties and those points placed in the solid region was given the solid polyurethane foam material properties while those in the cellular region was assigned with the cellular polyurethane foam material property(Shim et al., 2008). This allowed our model to have location dependent cortical thickness.

The contact between the femoral head and the acetabulum was modeled as frictional contact ($\mu = 0.3$) and the boundary conditions used in FE simulation were the same as the experiment. The nodes on the superior region of the iliac crest were fixed and two different loading conditions used in the experiment were used as the boundary condition. As in the experiment, the standing and seating positions were differentiated by varying the angle α defined in Figure 10. A vertically directed force was exerted on the femoral head mesh until failure.

The failure behaviour was characterized using the distortion energy (DE) theory of failure (Keyak et al., 1997). The DE theory is a simplified form of the Hoffman failure theory which was proposed for brittle fracture of orthotropic materials (Hoffman, 1967). Assuming isotropy, the fracture condition is reduced to the following (Lotz et al., 1991)

$$C_1\left[\sigma_2-\sigma_3\right]^2+C_2\left[\sigma_3-\sigma_1\right]^2+C_3\left[\sigma_1-\sigma_2\right]^2+C_4\sigma_1+C_5\sigma_2+C_6\sigma_3=1 \quad (1)$$

where

$$C_1=C_2=C_3=\frac{1}{2S_tS_c}$$

$$C_4=C_5=C_6=\frac{1}{S_t}-\frac{1}{S_c}$$

In this equation, σ_i is the principal stresses and S_t is the tensile strength and Sc is the compressive strength. If S_t and S_c are equal, Equation (1) becomes the distortion energy (DE) theory of failure, which was used in our study as a failure criterion. Since we used Gauss points in assigning material properties, we calculated a factor of safety (FOS) for every Gauss point (Equation 2) and if the FOS value was predicted to be less than one the Gauss point was regarded as in failure (Keyak et al., 1997). The fracture load and location were recorded for each loading condition and compared with the experimental results.

$$FOS=\frac{Gauss\ point\ strength\ (from\ CT\ and\ material\ property)}{Gauss\ point\ von\ Mises\ stress\ (from\ FE\ simulation)} \quad (2)$$

4.2.3. Finite element model sensitivity analysis

Sensitivity analysis was performed to find out which material parameters affect the strength of the pelvic bone most. The parameters of interest for sensitivity analysis were: 1) cortical thickness; 2) cortical modulus; 3) trabecular modulus. Since we used synthetic bones made of polyurethane foam, the three corresponding material parameters for the Sawbone FE model were 1) solid polyurethane foam thickness; 2) solid polyurethane modulus; 3) cellular polyurethane modulus. The values for the parameters were varied to see their effects on the predicted fracture load. The following equation (Equation 3) was used to measure the sensitivity of the chosen parameters.

$$S=\frac{\%\ Change\ in\ predicted\ fracture\ load}{\%\ Change\ in\ input\ parameter} \quad (3)$$

The range of simulated variation in the input parameters is given in Table 3. Since we used Gauss points in assigning material properties, the number of Gauss points in the transverse direction was varied from 4 to 6, which had the equivalent effect of varying the solid polyurethane thickness by -40% to +50% (Shim et al., 2008). As for the modulus values, the values were varied by ±25%, which was the next available value in the manufacturer's specification for material properties (Table 3). Multiple FE simulations were run with these values and the change in the predicted fracture load was recorded.

	Simulated of variation
Solid polyurethane foam thickness	-40% and +50% from the original thickness obtained from CT scans
Solid polyurethane foam modulus	±25 % from the original density value of 0.32g/cc
Cellular polyurethane foam modulus	±25% from the original density 0.16 g/cc

Table 3. Sensitivity analysis of polyurethane foam thickness and modulus

4.2.4. Fracture experiment with PU-foam pelvis and corresponding FE model predictions

The fracture behaviour of Sawbone pelves was linear elastic fracture of brittle material (Figure 12 (a)), which coincides with other studies involving fractures of polyurethane (Mcintyre and Anderston, 1979)

The fracture loads from the mechanical experiments are given in Figure 12 (b). The standing case has a slightly higher fracture load (mean 3400N) than the seating case (mean 2600N). Our FE model predicted the fracture load for both cases with a good accuracy as the predicted values are within the standard deviation of the experimental values for both case (Figure 12). The predicted fracture loads from the FE model are 3200N and 2300N for standing and seating cases respectively.

The predicted and actual fracture locations were consistent for both experiments and FE simulations and the fractures occurred mainly in the posterior region of the acetabulum. Different fracture patterns were obtained from two different loading conditions. For the fall from standing experiment, the fracture pattern resembled posterior column fracture according to the Letournel's classification (Letournel, 1980) while the dashboard experiment produced posterior wall fractures. Since the main cause of posterior wall fracture is car accidents (Spagnolo et al., 2009), our experimental set-up was able to capture the main features present in this fracture. The fracture locations predicted by the FE model were similar to the actual fracture patterns from the experiment. For the fall from heights fracture case, the failed Gauss points were concentrated at the region that extends from the dome of the acetabulum to the posterior superior region and then to the posterior column of the pelvis. This resembled the posterior column fracture that was observed from the experiment. For the seating case, on the other hand, the failed Gauss points were more or less limited in the posterior wall region of the acetabular rim, resembling the posterior wall fracture (Figure 12 (a)).

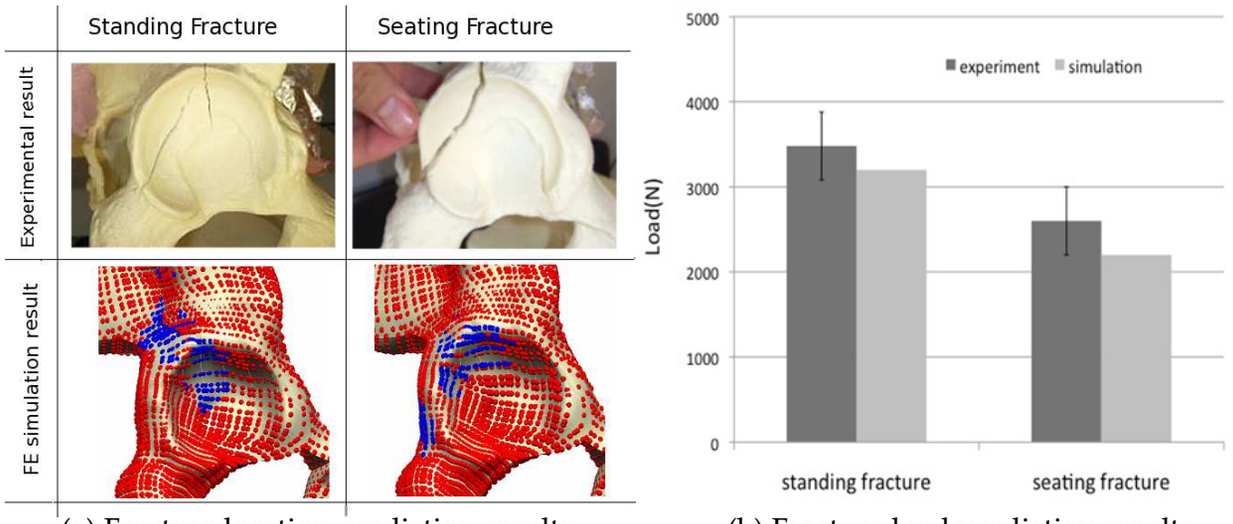

(a) Fracture location prediction results (b) Fracture load prediction results

Figure 12. Fracture location (a) and load (b) predictions from FE models

Once the fracture prediction was done, the sensitivity analysis was performed. Three input parameters (solid polyurethane thickness and modulus, cellular polyurethane modulus) were varied to examine the effect of their variation on the predicted fracture load. Among the three input parameters solid polyurethane foam modulus had the greatest impact on the resulting fracture load. Solid polyurethane foam thickness also had some effect on the predicted fracture load, but the sensitivity of this parameter was not as high as the modulus. Cellular polyurethane foam modulus, on the other hand, did not have any significant impact on the predicted fracture load as can be seen in Table 4. Since the pelvis has a sandwich structure where the outer cortical shell bears most of the load, our results indicate that this structural characteristic is also preserved even when the pelvis undergoes fracture.

Type of input parameters	Amount of variations in input parameters	Predicted fracture load	Sensitivity
Solid polyurethane foam thickness	0.6	3200	0.395
	1.4	4500	0.461
Solid polyurethane foam Modulus	153	2200	0.858
	400	5000	0.874
Cellular polyurethane foam Modulus	12.4	3200	0.128
	47.5	3500	0.028

Table 4. Results of sensitivity analysis

4.2.5. Feasibility of the use of synthetic PU-based bone in validating FE fracture predictions

FE models have been extensively used in predicting fracture load. Our approach to fracture mechanics was based on the work by Keyak and co-workers (Keyak et al., 1997, Korn et al.,

2001) which used the DE theory of fracture as well as material non-linearity. However, our approach differs from their work in that we simulated acetabular fractures not fractures of the proximal femur which are generally more complicated than fractures of the proximal femur. Moreover, rather than applying force directly to the bone of interest as done in majority of the FE fracture studies, we employed a contact mechanics approach where the force was applied to the acetabulum via the femoral head. Another novel approach of our study is that we incorporated geometric non-linearity to the model by using full finite elasticity governing equations, which has been found to enhance the fracture prediction capabilities of FE models (St^lken and Kinney, 2003).

However the most notable feature of our approach is the use of PU-based synthetic bone in validating FE fracture predictions. At present, it is not known whether our model can predict human bone fractures with the same degree of accuracy as the synthetic bones. Therefore caution is required when interpreting the data. However we are confident that our result will translate into human bones due to the following reasons. Firstly our experimental results with PU-foam pelves showed similar results as other human cadaver results as the fracture patterns generated in seating and standing cases correspond well with clinical results. Moreover the sensitivity analysis revealed that our model behaves in a similar manner as the cadaver bones despite the apparent difference in absolute magnitudes in modulus values between PU-foams and bones.

In fact, PU-foam based synthetic bone served our purpose of model validation very well due to their uniformity and consistency (Nabavi et al., 2009). As such, the ASTM standard states that it is "an ideal material for comparative testing" of various orthopaedic devices (American Society for Testing and Materials, 2008b). Although the fracture load is expected to be different from the fracture load of human pelvis, the material behaviour is expected to be comparable to human bones, both of which exhibit brittle fracture (Schileo et al., 2008, Thompson et al., 2003). Therefore the model's ability to predict fracture load and location of the synthetic bone can be regarded as a positive indication that it will also be applicable to human cases. Therefore we continued to use this approach in developing and validating FE model predictions for fracture stability with PU-foam based synthetic bones, which will be described in the next section(Shim et al., 2011).

4.3. Development and validation of finite element predictions of the stability of fracture fixation with PU-foam based synthetic bones

The posterior wall fracture is the most common fracture type of the acetabulum(Baumgaertner, 1999). Depending on the fragment size, open reduction and internal fixation (ORIF) is performed especially when the fracture involves more than 50% of the posterior wall. But ORIF requires considerable exposure that often leads to major blood loss and significant complications(Shuler et al., 1995). Percutaneous screw fixations, on the other hand, have become an attractive treatment option as they minimize exposure, blood loss and risk of infection. As such, they have been advocated by some authors

(Parker and Copeland, 1997) for the treatment of minimally displaced acetabular fractures without comminution or free fragment in the joint. However the biomechanical stability of percutaneous fixation has not been studied thoroughly, especially in terms of interfragmentary movement. In particular, the stability of percutaneous fixation in acetabular fractures has not been compared with the more conventional ORIF involving a plate with screws. There have been previous biomechanical studies that compared different types of stabilization in posterior wall fractures (Goulet et al., 1994, Zoys et al., 1999). But the main focus of such studies was to compare the strength of several types of osteosynthesis. However it is interfragmentary movement that exerts major influences on the primary stability and fracture healing (Klein et al., 2003, Wehner et al., 2010). As discussed in Section 3, PU-foam based synthetic bones have been used extensively in testing stability of various osteosynthesis techniques. Therefore we have further developed our FE model capable of prediction acetabular fractures to simulate stability in osteosynthesis. Specifically, we have developed a fast and efficient way of predicting the interfragmentary movement in percutaneous fixation of posterior wall fractures of the acetabulum and validated with a matching biomechanical experiment using PU-foam based synthetic pelves.

4.3.1. Mechanical experiment with PU-foam based synthetic pelvis

Seven synthetic pelves (Full Male Pelvis 1301-1, Pacific Research Laboratories Inc) were loaded until failure with the loading condition that resembled seating fracture[10], creating posterior wall fractures[11]. The fractures were then reduced and fixed with two fixation methods –with two screws (3.5mm Titan Screws, Synthes) and then with a 10-12 hole plates (3.5mm Titan Reconstruction- or LCDC-Plates, Synthes) by an experienced surgeon (JB) (Figure 13 A and B). The maximum remaining crack was 0.7 mm.

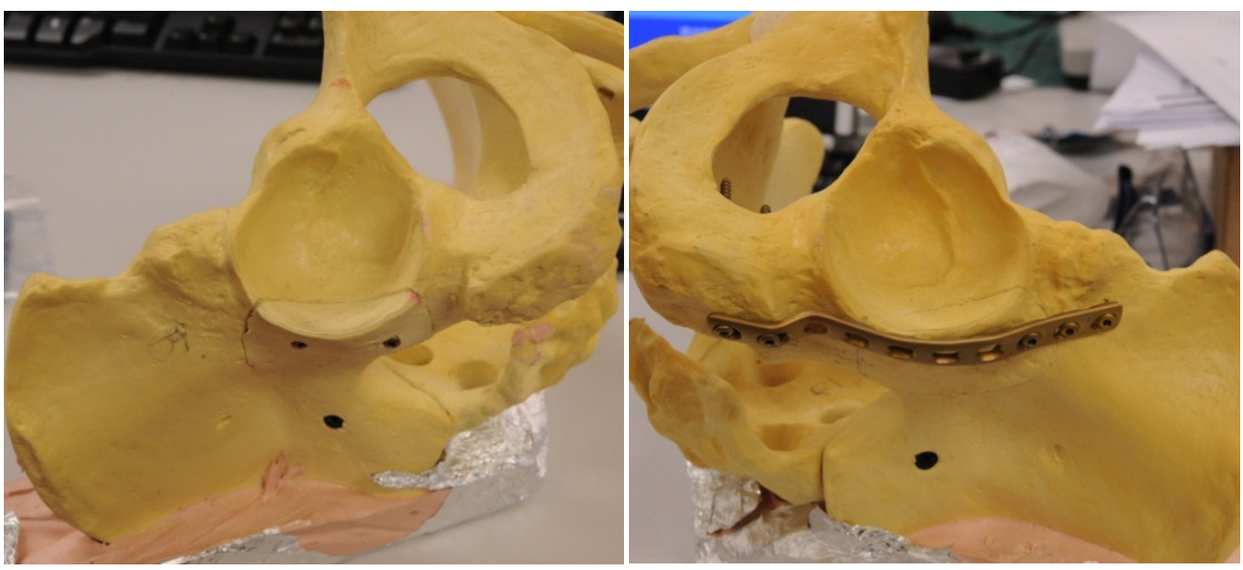

(a) Screw fixation (b) Plate fixation

Figure 13. Two fixation methods performed on the fractured acetabulum

The pelves were then loaded in the Instron Machine (Instron 5800 series) with a cyclic load that oscillated between 0N to 900N at 40N/s. The force was applied using a synthetic femoral head (Large Left Femur, 1129, Pacific Research Laboratories Inc) attached to the crosshead of the Instron Machine (Figure 14). At the multiple of 300N the loading was paused for 3 seconds to measure the displacement between the fragment and the bone by taking photographs of the crack opening (Figure 14 (a)). A digital SLR camera (Nikon D70) with a 50mm macro lens (NIKKOR dental lens) was used to accurately measure the amount of crack openings (resolution of 10 μm (Figure 14 (b))). A resolution of 10μm was achieved (Figure 15).

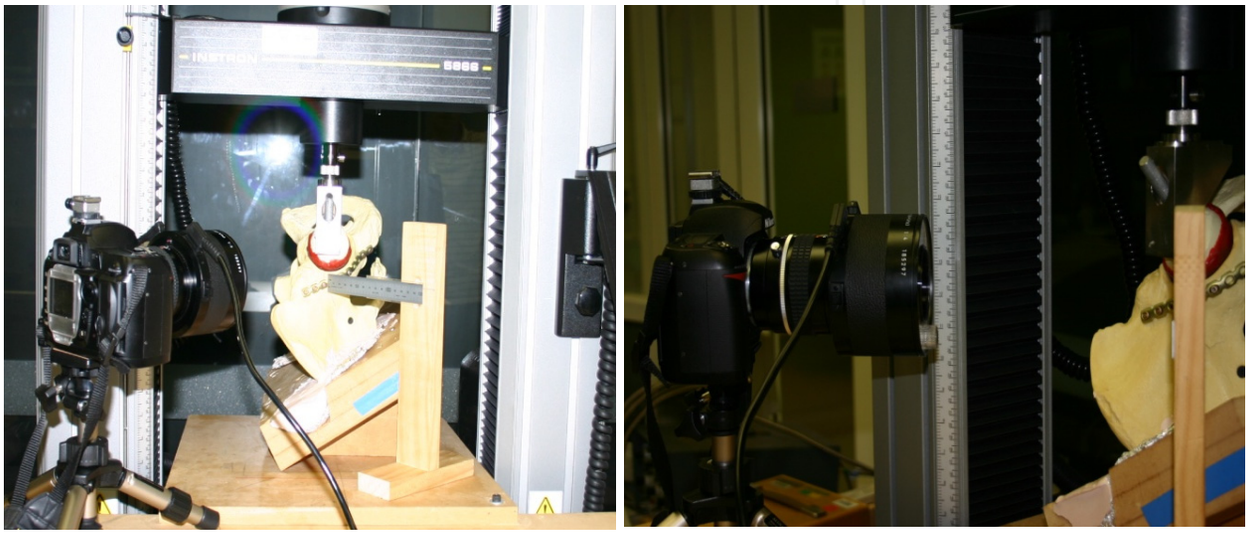

(a) Measurement set-up (b) Optical set-up with macro

Figure 14. Interfragmentary movement measuring set-up with a digital single-lens reflex camera and an Instron machine

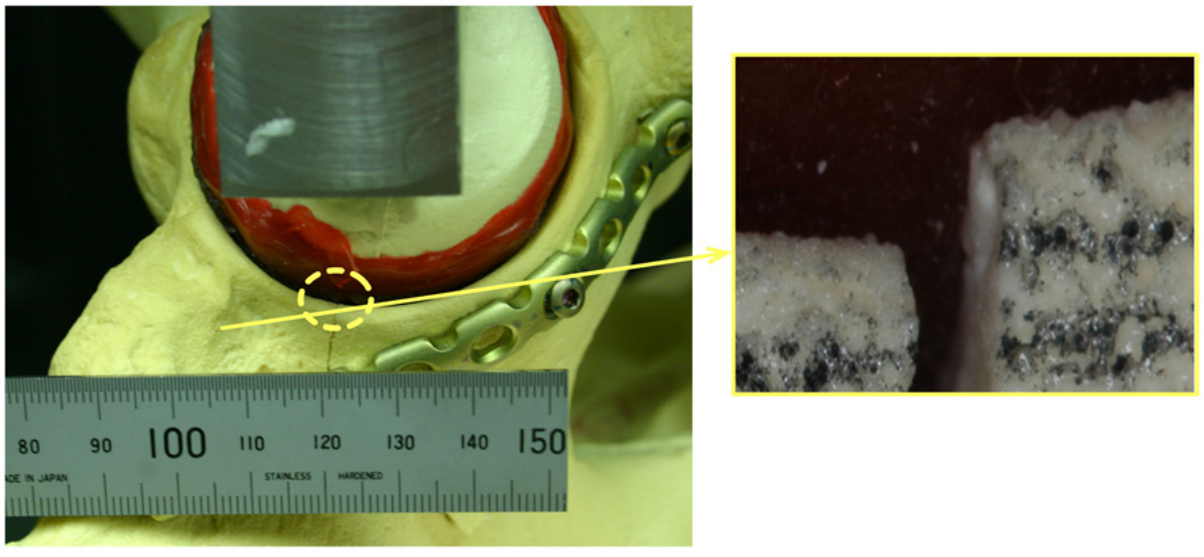

Figure 15. A photo taken with the macro lens. The magnified view shown in the box left has the resolution of 10μm

The displacement was measured in two different positions – front and side - to obtain the fragment movement in three directions – frontal, vertical and lateral directions (Figure 16). 10 photographs were taken at each angle and load and the mean value was taken.

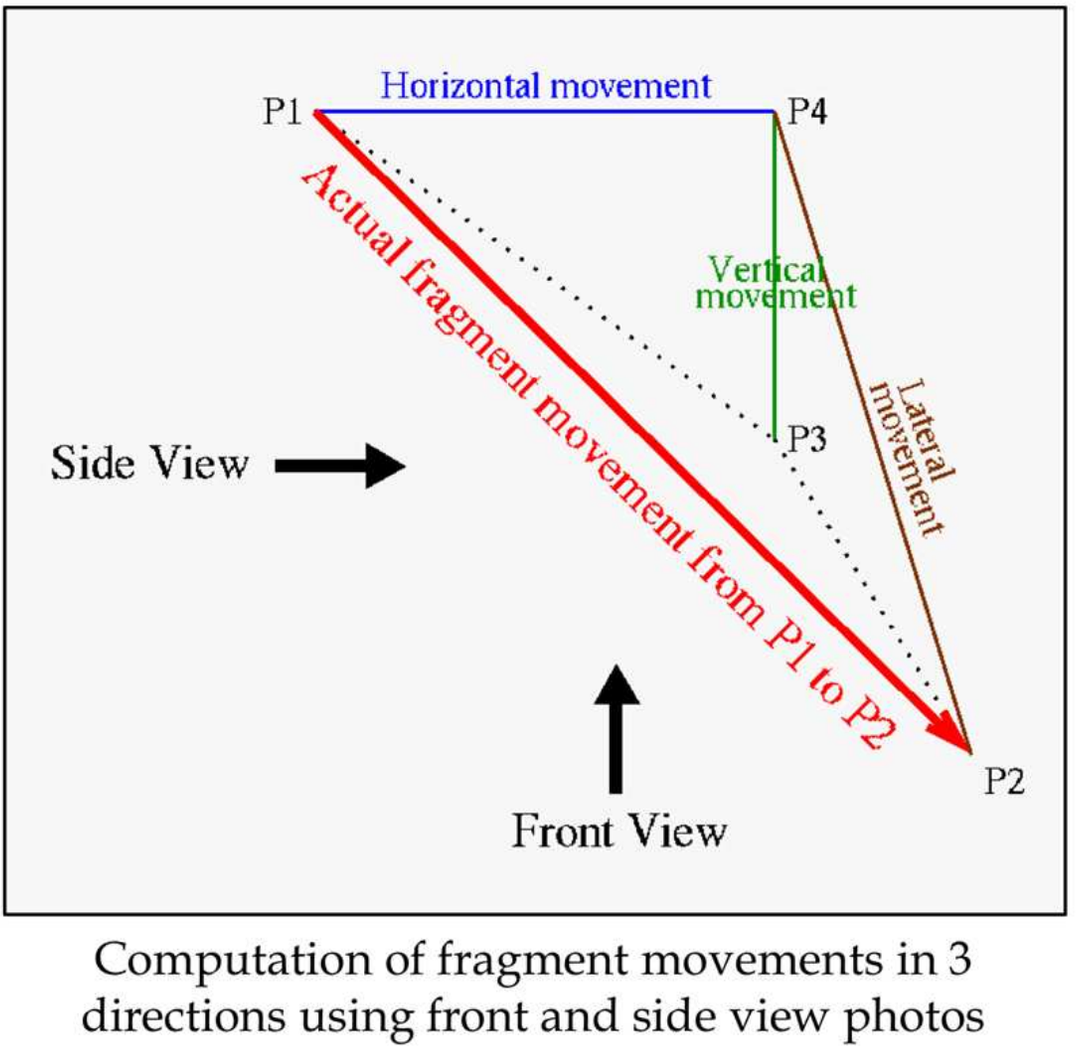

Figure 16. Getting fragment movements in three directions – horizontal, vertical and lateral – using photos taken at two different views. The actual movement of the fragment is from P1 to P2 from no load to full load conditions. The front view photo gives the triangle P1P4P3, allowing us to calculate horizontal and vertical movement. The side view photo gives the triangle P4P2P3 which allows us to calculate the lateral movement.

4.3.2. Finite element simulation

The stability of screw fixation was analyzed with finite element models. We developed the models of the fractured pelvis, fragment and femoral head in order to perform the mechanical testing that we did in silico. Firstly, one of the PU-foam based synthetic fractured pelves that had been fixed with two screws was dismantled. The resulting fractured pelvis and its fragment were scanned separately with a Faro Arm (Siler Series Faro Arm) and a laser scanner (Model Maker H40 Laser Scanner). Two sets of data point

clouds, which accurately described the shapes of the fragment and the fractured pelvis, were obtained (Figure 17). The fractured pelvis model was developed from our previous FE model of the pelvis, which was generated from CT scans of the synthetic pelvis used in the experiment (Shim et al., 2010) . Our elements had inhomogeneous location dependent material properties despite large element size and different material properties were assigned to solid and cellular polyurethane foams which mimic cortical and cancellous bone properties separately. The loading and boundary condition that mimics the mechanical experiment setup were employed. The FE models of the screws were not generated explicitly. Instead tied contact was used to model the bond between the fractured pelvis and the fragment from the screws. The locations of the screws on the fragment FE model were identified first from the laser scanned data. Then, the tied contact condition that ensures a perfect bond between slave and master faces was imposed on the identified faces to simulate the bond that screws provide when connecting the fragment with the bone. The rest of fragment faces were modeled with frictional contact (μ=0.4)(Gordon et al., 1989). The predicted interfragmentary movements from the FE model under the same loading and boundary conditions as the experiment were then compared with the experimental value to test our hypothesis. Once tested, then, the screw positions were varied by changing tied contact faces to simulate all possible screw positions in order to identify the positions that achieved the most stable fixation.

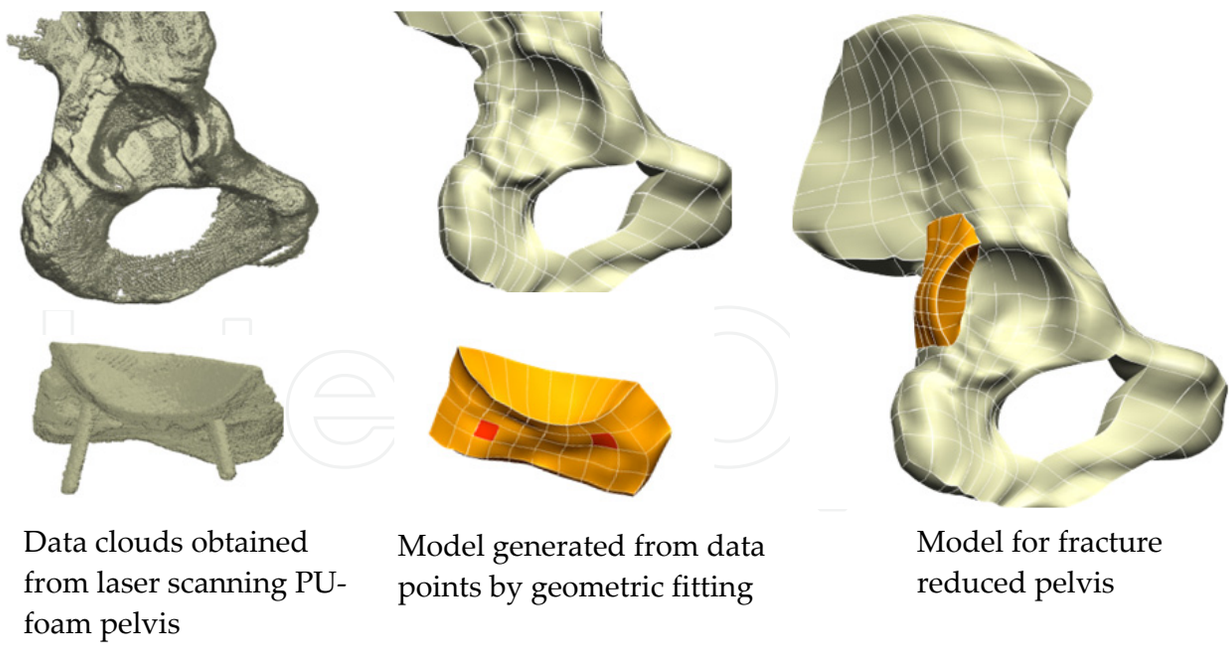

Figure 17. The far left column shows clouds of data points obtained from laser scanning. The center column shows the meshes for the fragment and fractured pelvis that were generated by geometric fitting to laser scanned data points. The red faces on the fragment mesh indicate where tied contact conditions were imposed in order to simulate the support provided by the screws. The final mesh is shown on the far right column.

4.3.3. Interfragmentary movement in acetabular fracture osteosynthesis measured with PU- foam based synthetic bones

The overall amount of displacement between the pelvis and the fragment was relatively small and the main direction of the fragment movement was in the lateral posterior direction (in body directions). The average displacement was around 0.4 – 0.9 mm for both screw and plate fixations. The plates gave higher stability especially in the horizontal and lateral directions (Figure 18). However, screw fixations also gave good stability of less than 1mm on average in all directions. Therefore, considering the fact that the maximum load of our experiment was higher than normally allowed weight bearing (around 20kg after the surgery for 3 months), the stability of screw fixation was sufficient for the cyclic loading condition used.

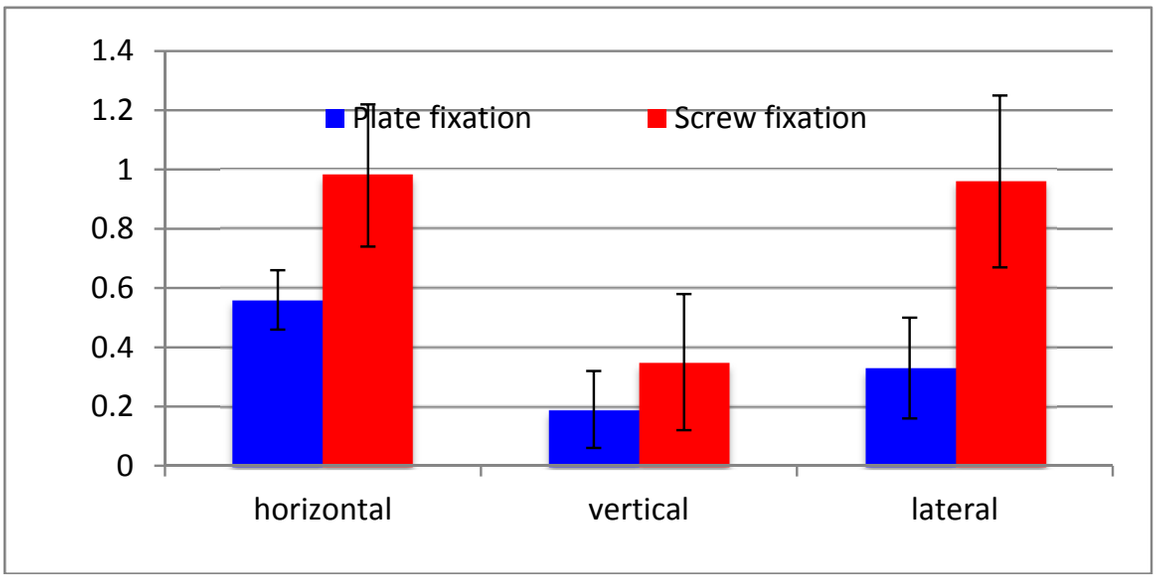

Figure 18. Comparison of interfragmentary movement between plate and screw fixation

4.3.4. Accuracy of FE model interfragmentary movement predictions validated with PU-foam based synthetic bones

The FE model predicted the movement of the fragment in screw fixations with a good accuracy. The values predicted by the FE simulation were within one standard deviation of the experimental measurements (Figure 19) in the horizontal and lateral directions. The predicted vertical direction movement was a little bit greater than the upper limit of the experimental measurement (mean + 1 SD) but still very close to it as the difference was 0.05 mm.

The optimized screw positions were found to be on the two diagonal corners of the fragment. When the virtual screws were placed in this manner, the stability of screw fixations improved dramatically to the level that is comparable to plate fixation (Figure 20). The fragment movements in the horizontal and lateral directions were smaller than the average movements in the plate fixation in these directions. Although the movement in the vertical direction was bigger than the upper limit of the experimental measurement, the difference was small 0.1mm.

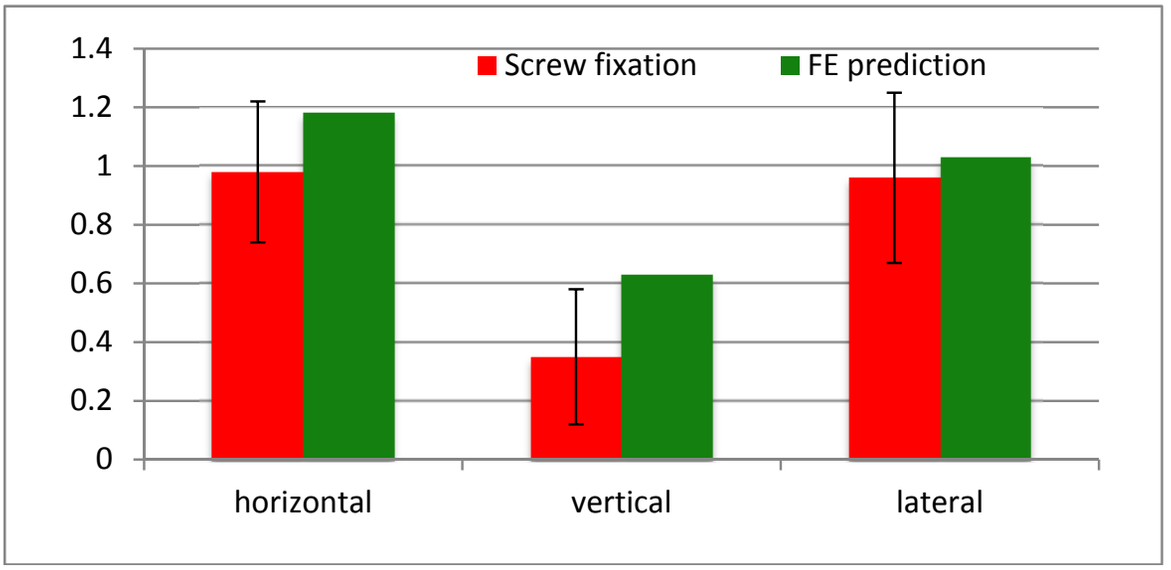

Figure 19. Comparison between FE prediction and experimental measurement

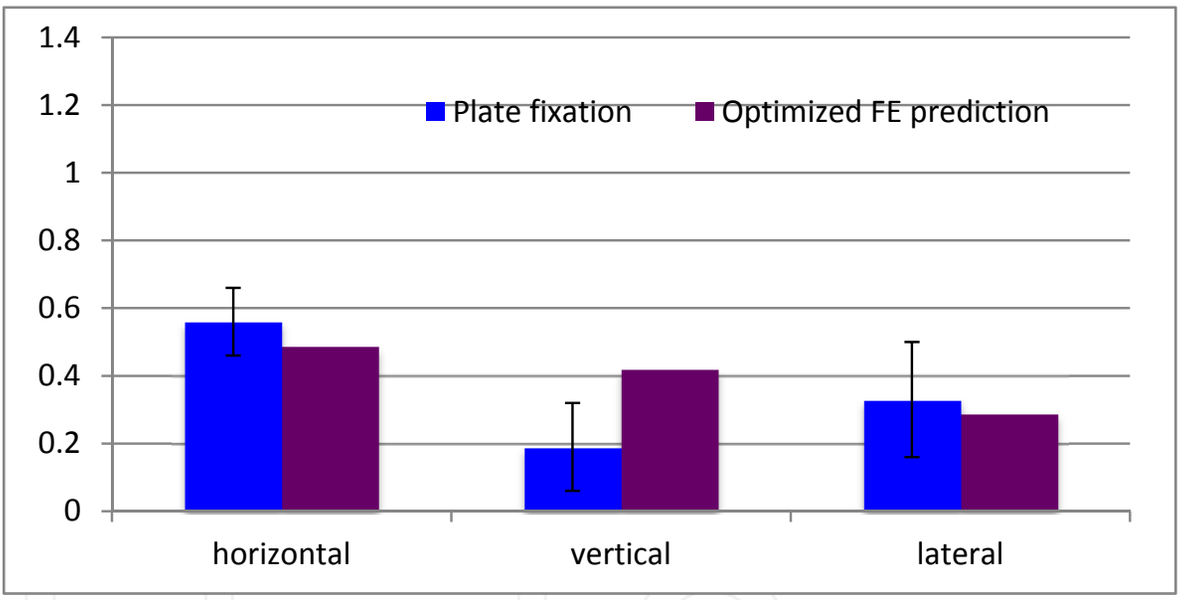

Figure 20. Comparison between plate fixation and optimized screw fixation predicted from FE model

4.3.5. Feasibility of the use of synthetic PU-foam based bone in validating FE predictions of fracture stability

We have developed a new and efficient way of simulating interfragmentary movement in acetabular fractures using a FE model. We validated our method with a biomechanical experiment involving PU-foam based synthetic bones. There are numerous studies that employed PU-foam based synthetic bones in measuring fracture stability as discussed in Section 3. However this data has not been used in validating FE model predictions of fracture stability. The use of FE models in fracture analysis is not new. However, the major focus has been to analyze the stress distribution on the implant or the overall stiffness of bone/implant composite after fracture fixation (Eberle et al., 2009, Stoffel et al., 2003).

Therefore we have performed a biomechanical experiment with PU-foam based synthetic bones to measure interfragmentary movements in 3D and used the result to validate our FE model.

The mechanical experiment with synthetic pelves showed that the displacement between fragment and bone was relatively small for both plate and screw fixations, indicating that screw fixations in single fragment fractures may be a good alternative to the current gold standard of plate fixation. In particular the excellent stability displayed by the screw FE model with the optimized screw positions indicate that screw fixations along with computer navigation should be an option considered by trauma surgeons if available.

The FE model showed a great potential for use in analyzing fracture fixation techniques. Our model was able to predict the movement of the fragment with a reasonable accuracy. Although we have not modeled screws explicitly, our modeling approach was able to accurately predict the fragment movement, which was the main aim of the model. Moreover the computational efficiency of the approach allowed us to perform a parametric study for optimization of screw positions.

Since we have used PU-foam based synthetic pelves in our study it is not known if our model predictions will be as accurate when cadaver bones are used. However the use of synthetic bones has some advantages due to their uniformity and consistency (Nabavi et al., 2009). Moreover the main aim was to make comparisons between different osteosynthesis techniques and between experimental and FE simulations and the ASTM standard states that it is "an ideal material for comparative testing (American Society for Testing and Materials, 2008a)." In this regard, the use of PU-foam based synthetic bones in comparative studies in orthopaedic biomechanics can provide useful data for FE model validation as well as testing hypothesis.

5. Concluding remarks

In this chapter we discussed the use of polyurethane in orthopaedic biomechanical experiments. Due to the similarity of polyurethane foam with cancellous bone in terms of microstructure and material properties, polyurethane has found a unique and important position in orthopaedic biomechanics studies. The main use of PU-foams was in experimental studies to find optimum values in various surgical procedures and to test stability of fracture or joint replacement implants. Due to the uniformity and consistency in material properties, PU-foam based synthetic bones are capable of generating reproducible results that are so difficult to obtain when using human cadaver bones. Therefore we used PU-foam materials in designing bone graft harvesters and obtaining validation data for FE model predictions in fracture load and stability. Although material properties of PU-foams are not identical to natural bone, they are able to generate comparable results that can provide important insight into surgical procedures or function of implants or devices. Moreover thanks to the advent of new composite bones made up of PU-foams and other relevant materials that mimic the geometry, structure and material properties of human

bone, only the imagination of biomechanical engineers is the limit in ways that PU-foam based materials can be used in orthopaedic biomechanical studies in the future.

Author details

V. Shim and I. Anderson
Auckland Bioengineering Institute, University of Auckland, New Zealand

J. Boheme and C. Josten
University of Leipzig, Germany

Acknowledgement

This work was supported in part by Faculty Development Research Fund (FRDF) from the University of Auckland awarded to V. Shim and Federal Ministry of Education and Research (BMBF) grant awarded to J. Böhme. The authors would like to thank Mr. Sharif Malak for his work in orthogonal cutting of PU-foams.

6. References

Acevedo, J. I., Sammarco, V. J., Boucher, H. R., Parks, B. G., Schon, L. C. & Myerson, M. S. (2002) Mechanical comparison of cyclic loading in five different first metatarsal shaft osteotomies. *Foot Ankle Int,* 23, 711-6.

Agneskirchner, J. D., Freiling, D., Hurschler, C. & Lobenhoffer, P. (2006) Primary stability of four different implants for opening wedge high tibial osteotomy. *Knee Surg Sports Traumatol Arthrosc,* 14, 291-300.

American Society for Testing and Materials, A. (2008a) ASTM F1839 - 08 standard Specification for Rigid Polyurethane Foam for Use as a Standard Material for Testing Orthopedic Devices and Instruments.

American Society for Testing and Materials, A. (2008b) ASTM F1839 - 08 standard Specification for Rigid Polyurethane Foam for Use as a Standard Material for Testing Orthopedic Devices and Instruments.

Arrington, E. D., Smith, W. J., Chambers, H. G., Bucknell, A. L. & Davino, N. A. (1996) Complications of iliac crest bone graft harvesting. *Clin Orthop Relat Res*, 300-9.

Baumgaertner, M. R. (1999) Fractures of the posterior wall of the acetabulum. *J Am Acad Orthop Surg,* 7, 54-65.

Betz, R. R. (2002) Limitations of autograft and allograft: new synthetic solutions. *Orthopedics,* 25, s561-70.

Borrelli, J., JR., Ricci, W. M., Steger-May, K., Totty, W. G. & Goldfarb, C. (2005) Postoperative radiographic assessment of acetabular fractures: a comparison of plain radiographs and CT scans. *J Orthop Trauma,* 19, 299-304.

Bredbenner, T. L. & Haug, R. H. (2000) Substitutes for human cadaveric bone in maxillofacial rigid fixation research. *Oral Surg Oral Med Oral Pathol Oral Radiol Endod,* 90, 574-80.

Burstein, F. D., Simms, C., Cohen, S. R., Work, F. & Paschal, M. (2000) Iliac crest bone graft harvesting techniques: a comparison. *Plast Reconstr Surg,* 105, 34-9.

Caglar, Y. S., Torun, F., Pait, T. G., Hogue, W., Bozkurt, M. & Ozgen, S. (2005) Biomechanical comparison of inside-outside screws, cables, and regular screws, using a sawbone model. *Neurosurg Rev,* 28, 53-8.

Calvert, K. L., Trumble, K. P., Webster, T. J. & Kirkpatrick, L. A. Characterization of commercial rigid polyurethane foams used as bone analogs for implant testing. *J Mater Sci Mater Med,* 21, 1453-61.

Chong, A. C., Friis, E. A., Ballard, G. P., Czuwala, P. J. & Cooke, F. W. (2007a) Fatigue performance of composite analogue femur constructs under high activity loading. *Ann Biomed Eng,* 35, 1196-205.

Chong, A. C., Miller, F., Buxton, M. & Friis, E. A. (2007b) Fracture toughness and fatigue crack propagation rate of short fiber reinforced epoxy composites for analogue cortical bone. *J Biomech Eng,* 129, 487-93.

Cole, J. D. & Bolhofner, B. R. (1994) Acetabular fracture fixation via a modified Stoppa limited intrapelvic approach. Description of operative technique and preliminary treatment results. *Clin Orthop Relat Res*, 112-23.

Cristofolini, L., Teutonico, A. S., Monti, L., Cappello, A. & Toni, A. (2003) Comparative in vitro study on the long term performance of cemented hip stems: validation of a protocol to discriminate between "good" and "bad" designs. *J Biomech,* 36, 1603-15.

Eberle, S., Gerber, C., Von Oldenburg, G., Hungerer, S. & AUGAT, P. (2009) Type of hip fracture determines load share in intramedullary osteosynthesis. *Clin Orthop Relat Res,* 467, 1972-80.

Farshad, M., Weinert-Aplin, R. A., Stalder, M., Koch, P. P., Snedeker, J. G. & Meyer, D. C. (2011) Embossing of a screw thread and TCP granules enhances the fixation strength of compressed ACL grafts with interference screws. *Knee Surg Sports Traumatol Arthrosc*.

Giannoudis, P. V., Grotz, M. R., Papakostidis, C. & Dinopoulos, H. (2005) Operative treatment of displaced fractures of the acetabulum. A meta-analysis. *J Bone Joint Surg Br,* 87, 2-9.

Gibson, L. J. & Ashby, M. F. (1988) *Cellular Solids - Structure and properties,* Oxford, Pergamon Press.

Gordon, J., Kauzlarich, J. J. & Thacker, J. G. (1989) Tests of two new polyurethane foam wheelchair tires. *J Rehabil Res Dev,* 26, 33-46.

Goulet, J. A., Rouleau, J. P., Mason, D. J. & Goldstein, S. A. (1994) Comminuted fractures of the posterior wall of the acetabulum. A biomechanical evaluation of fixation methods. *J Bone Joint Surg Am,* 76, 1457-63.

Gulsen, M., Karatosun, V. & Uyulgan, B. The biomechanical assessment of fixation methods in periprosthetic femur fractures. *Acta Orthop Traumatol Turc,* 45, 266-9.

Heiner, A. D. (2008) Structural properties of fourth-generation composite femurs and tibias. *J Biomech,* 41, 3282-4.

Hoffman, O. (1967) The Brittle Strength of Orthotropic Materials. *J. Composite Materials,* 1, 200-206.

Jacobs, C. H., Pope, M. H., Berry, J. T. & Hoaglund, F. (1974) A study of the bone machining process-orthogonal cutting. *J Biomech,* 7, 131-6.

Keyak, J. H. (2001) Improved prediction of proximal femoral fracture load using nonlinear finite element models. *Medical Engineering and Physics,* 23, 165-173.

Keyak, J. H., Rossi, S. A., Jones, K. A. & Skinner, H. B. (1997) Prediction of femoral fracture load using automated finite element modeling. *Journal of Biomechanics,* 31, 125-133.

Klein, P., Schell, H., Streitparth, F., Heller, M., Kassi, J. P., Kandziora, F., Bragulla, H., Haas, N. P. & Duda, G. N. (2003) The initial phase of fracture healing is specifically sensitive to mechanical conditions. *J Orthop Res,* 21, 662-9.

Konrath, G. A., Hamel, A. J., Sharkey, N. A., Bay, B. & Olson, S. A. (1998a) Biomechanical evaluation of a low anterior wall fracture: correlation with the CT subchondral arc. *J Orthop Trauma,* 12, 152-8.

Konrath, G. A., Hamel, A. J., Sharkey, N. A., Bay, B. K. & Olson, S. A. (1998b) Biomechanical consequences of anterior column fracture of the acetabulum. *J Orthop Trauma,* 12, 547-52.

Korn, B., Weissman, S., Werner, T. & Gardiner, K. (2001) Report on the tenth international workshop on the identification of transcribed sequences 2000. Heidelberg, Germany, October 28-31, 2000. *Cytogenet Cell Genet,* 92, 49-58.

Krause, W. R., Bradbury, D. W., Kelly, J. E. & Lunceford, E. M. (1982) Temperature elevations in orthopaedic cutting operations. *J Biomech,* 15, 267-75.

Krenn, M. H., Piotrowski, W. P., Penzkofer, R. & Augat, P. (2008) Influence of thread design on pedicle screw fixation. Laboratory investigation. *J Neurosurg Spine,* 9, 90-5.

Kurz, L. T., Garfin, S. R. & Booth, R. E., JR. (1989) Harvesting autogenous iliac bone grafts. A review of complications and techniques. *Spine (Phila Pa 1976),* 14, 1324-31.

Letournel, E. (1980) Acetabulum fractures: classicifaction and management. *Clin Orthop Relat Res,* 151, 81-106.

Lewandrowski, K. U., Gresser, J. D., Bondre, S., Silva, A. E., Wise, D. L. & Trantolo, D. J. (2000) Developing porosity of poly(propylene glycol-co-fumaric acid) bone graft substitutes and the effect on osteointegration: a preliminary histology study in rats. *J Biomater Sci Polym Ed,* 11, 879-89.

Lotz, J. C., Cheal, E. J. & Hayes, W. C. (1991) Fracture prediction for proximal femur using finite element models: Part II - Nonlinear analysis. *Journal of Biomechanical Engineering,* 113, 361-365.

Malak, S. F. & Anderson, I. A. (2008) Orthogonal cutting of cancellous bone with application to the harvesting of bone autograft. *Med Eng Phys,* 30, 717-24.

Malak, S. F. F. & Anderson, I. A. (2005) Orthogonal cutting of polyurethane foam. *International Journal of Mechanical Sciences,* 47, 867-883.

Mcintyre, A. & Anderston, E. (1979) Fracture properties of a rigid polyurethane foam over a range of densities. *Polymer,* 20, 247-253.

Melamed, E. A., Schon, L. C., Myerson, M. S. & Parks, B. G. (2002) Two modifications of the Weil osteotomy: analysis on sawbone models. *Foot Ankle Int,* 23, 400-5.

Nabavi, A., Yeoh, K. M., Shidiac, L., Appleyard, R., Gillies, R. M. & Turnbull, A. (2009) Effects of positioning and notching of resurfaced femurs on femoral neck strength: a biomechanical test. *Journal of orthopaedic surgery,* 17, 47-50.

Nasson, S., Shuff, C., Palmer, D., Owen, J., Wayne, J., Carr, J., Adelaar, R. & May, D. (2001) Biomechanical comparison of ankle arthrodesis techniques: crossed screws vs. blade plate. *Foot Ankle Int,* 22, 575-80.

Natali, C., Ingle, P. & Dowell, J. (1996) Orthopaedic bone drills-can they be improved? Temperature changes near the drilling face. *J Bone Joint Surg Br,* 78, 357-62.

Nyska, M., Trnka, H. J., Parks, B. G. & Myerson, M. S. (2002) Proximal metatarsal osteotomies: a comparative geometric analysis conducted on sawbone models. *Foot Ankle Int,* 23, 938-45.

Olson, S. A., Kadrmas, M. W., Hernandez, J. D., Glisson, R. R. & WEST, J. L. (2007) Augmentation of posterior wall acetabular fracture fixation using calcium-phosphate cement: a biomechanical analysis. *J Orthop Trauma,* 21, 608-16.

Papini, M., Zdero, R., Schemitsch, E. H. & Zalzal, P. (2007) The biomechanics of human femurs in axial and torsional loading: comparison of finite element analysis, human cadaveric femurs, and synthetic femurs. *J Biomech Eng,* 129, 12-9.

Parker, P. J. & Copeland, C. (1997) Percutaneous fluroscopic screw fixation of acetabular fractures. *Injury,* 28, 597-600.

Ross, N., Tacconi, L. & Miles, J. B. (2000) Heterotopic bone formation causing recurrent donor site pain following iliac crest bone harvesting. *Br J Neurosurg,* 14, 476-9.

Ruedi, T. P., Buckley, R. E. & Moran, C., G (2007) *AO Principles of fracture management* Davos, Switzerland, AO Publishing.

Russell, J. L. & Block, J. E. (2000) Surgical harvesting of bone graft from the ilium: point of view. *Med Hypotheses,* 55, 474-9.

Saha, S., Pal, S. & Albright, J. A. (1982) Surgical drilling: design and performance of an improved drill. *J Biomech Eng,* 104, 245-52.

Schileo, E., Taddei, F., Cristofolini, L. & Viceconti, M. (2008) Subject-specific finite element models implementing a maximum principal strain criterion are able to estimate failure risk and fracture location on human femurs tested in vitro. *J Biomech,* 41, 356-67.

Shim, V., Bohme, J., Vaitl, P., Klima, S., Josten, C. & Anderson, I. (2010) Finite element analysis of acetabular fractures--development and validation with a synthetic pelvis. *J Biomech,* 43, 1635-9.

Shim, V. B., Boshme, J., Vaitl, P., Josten, C. & Anderson, I. A. (2011) An efficient and accurate prediction of the stability of percutaneous fixation of acetabular fractures with finite element simulation. *J Biomech Eng,* 133, 094501.

Shim, V. B., Pitto, R. P., Streicher, R. M., Hunter, P. J. & Anderson, I. A. (2007) The use of sparse CT datasets for auto-generating accurate FE models of the femur and pelvis. *Journal of Biomechanics,* 40, 26-35.

Shim, V. B., Pitto, R. P., Streicher, R. M., Hunter, P. J. & Anderson, I. A. (2008) Development and validation of patient-specific finite element models of the hemipelvis generated from a sparse CT data set. *Journal of Biomechanical Engineering,* 130, 051010.

Shin, H. C. & Yoon, Y. S. (2006) Bone temperature estimation during orthopaedic round bur milling operations. *J Biomech,* 39, 33-9.

Shuler, T. E., Boone, D. C., Gruen, G. S. & Peitzman, A. B. (1995) Percutaneous iliosacral screw fixation: early treatment for unstable posterior pelvic ring disruptions. *J Trauma,* 38, 453-8.

Silber, J. S., Anderson, D. G., Daffner, S. D., Brislin, B. T., Leland, J. M., Hilibrand, A. S., Vaccaro, A. R. & Albert, T. J. (2003) Donor site morbidity after anterior iliac crest bone harvest for single-level anterior cervical discectomy and fusion. *Spine (Phila Pa 1976),* 28, 134-9.

Simoes, J. A., Vaz, M. A., Blatcher, S. & Taylor, M. (2000) Influence of head constraint and muscle forces on the strain distribution within the intact femur. *Med Eng Phys,* 22, 453-9.

Spagnolo, R., Bonalumi, M., Pace, F. & Capitani, D. (2009) Minimal-invasive posterior approach in the treatment of the posterior wall fractures of the acetabulum. *Musculoskeletal Surgery,* 93, 9-13.

Stˆlken, J. S. & Kinney, J. H. (2003) On the importance of geometric nonlinearity in finite-element simulations of trabecular bone failure. *Bone,* 33, 494-504.

Stoffel, K., Dieter, U., Stachowiak, G., Gachter, A. & Kuster, M. S. (2003) Biomechanical testing of the LCP--how can stability in locked internal fixators be controlled? *Injury,* 34 Suppl 2, B11-9.

Szivek, J. A., Thomas, M. & Benjamin, J. B. (1993) Characterization of a synthetic foam as a model for human cancellous bone. *J Appl Biomater,* 4, 269-72.

Szivek, J. A., Thompson, J. D. & Benjamin, J. B. (1995) Characterization of three formulations of a synthetic foam as models for a range of human cancellous bone types. *J Appl Biomater,* 6, 125-8.

Thompson, M. S., McCarthy, I. D., Lidgren, L. & Ryd, L. (2003) Compressive and shear properties of commercially available polyurethane foams. *J Biomech Eng,* 125, 732-4.

Tile, M., Helfet, D. L. & Kellam, J. F. (Eds.) (2003) *Fractures of the pelvis and acetabulum,* Philadelphia, PA USA, Lippincott Williams & Wilkins.

Trnka, H. J., Nyska, M., Parks, B. G. & Myerson, M. S. (2001) Dorsiflexion contracture after the Weil osteotomy: results of cadaver study and three-dimensional analysis. *Foot Ankle Int,* 22, 47-50.

Wehner, T., Penzkofer, R., Augat, P., Claes, L. & Simon, U. (2010) Improvement of the shear fixation stability of intramedullary nailing. *Clin Biomech (Bristol, Avon),* 26, 147-51.

Zdero, R., Olsen, M., Bougherara, H. & Schemitsch, E. H. (2008) Cancellous bone screw purchase: a comparison of synthetic femurs, human femurs, and finite element analysis. *Proc Inst Mech Eng H,* 222, 1175-83.

Zdero, R., Rose, S., Schemitsch, E. H. & Papini, M. (2007) Cortical screw pullout strength and effective shear stress in synthetic third generation composite femurs. *J Biomech Eng,* 129, 289-93.

Zoys, G. N., Mcganity, P. L., Lanctot, D. R., Athanasiou, K. A. & Heckman, J. D. (1999) Biomechanical evaluation of fixation of posterior acetabular wall fractures. *J South Orthop Assoc,* 8, 254-60; discussion 260.